# NEAR SURFACE GEOPHYSICS FOR THE STRUCTURAL ANALYSIS OF A MINE ROCK PILE, NORTHERN NEW MEXICO[1]

Remke L. Van Dam[2], Luiza A. Gutierrez, Virginia T. McLemore, G. Ward Wilson, Jan M.H. Hendrickx, and Bruce M. Walker

**Abstract.** Recent concerns regarding the rock pile stability of a mine in northern New Mexico have lead to the instigation of a multi-disciplinary research program to investigate the pile characteristics and behavior. Geophysical techniques and 7 trenches were used to assess the internal structure of the material for the Goathill North rock pile. Electromagnetic (EM) induction and ground penetrating radar (GPR) methods were used to measure the spatial variability in electrical conductivity and to image the internal structures of the rock pile, respectively. Seven trenches were excavated for analysis of the stratigraphy.

The measurements show the characteristics of the top 5 to 8 meters of the rock pile. The electrical conductivities varied typically around 6 mS/m, but on the southwestern part of the rock pile anomalously high values up to 30 mS/m were found. These high values can be explained by a different texture, mineralogy or pore-water composition, or a higher water content. In this area the penetration depth of the GPR waves is significantly reduced and the reflection configuration is dominated by sub-horizontal reflections. In general, the GPR results have a character of reflectors whose dip directions and angles (maximum 30 degrees) reflect the rock-pile deposition. The trench data show excellent overlap with the GPR survey.

Additional key words: stratigraphy, geophysics, ground penetrating radar, electromagnetic induction, Questa molybdenum mine

---

[1] Paper was presented at the 2005 National Meeting of the American Society of Mining and Reclamation, June 19-23, 2005. Published by ASMR, 3134 Montavesta Rd., Lexington, KY 40502.

[2] Remke L. Van Dam is Postdoctoral Research Associate in Hydrology, New Mexico Tech, Socorro, NM 87801 (corresponding author e-mail: rvd@nmt.edu). Luiza A. Gutierrez is Mineral Engineering Graduate Student, New Mexico Tech, Socorro, NM 87801. Virginia T. McLemore is Senior Economic Geologist, New Mexico Bureau of Geology and Mineral Resources, New Mexico Tech, Socorro, NM 87801. G. Ward Wilson is Professor of Mining Engineering, The University of British Columbia, Vancouver, B.C., Canada V6T1Z4. Jan M.H. Hendrickx is Professor of Hydrology, New Mexico Tech, Socorro, NM 87801. Bruce M. Walker is Chief Geologist, Molycorp Inc., Questa, NM 87556.

## Introduction

Molycorp's Questa Division is a molybdenum mine near Taos in northern New Mexico, USA (Fig. 1). The mine is located on the western end of the Taos Range of the Sangre de Cristo Mountains and is bounded on the south by Red River and on the north by the mountain divides. The primary rock lithologies on the mine property are andesite flows, andesite-to-quartz latite porphyry flows, rhyolite tuff, and aplite porphyries. The mine began production in 1919 from underground workings. Removal of overburden for open-pit mining (with ore production between 1965 and 1981) began in 1964. Current mining operations have shifted towards underground block-cave mining methods.

During the open-pit period of mining, approximately 317.5 million metric tons of overburden rock were deposited as rock piles onto mountain slopes and into tributary valleys. The Questa rock piles were constructed mostly by haul truck end dumping in high, single lifts, which involves the dumping of rock over the edge of the hill slopes (URS Corporation, 2000). End dumping generally results in the segregation of materials with the finer-grained material at the top and coarser-grained material at the base. The resulting layers are at the angle of repose and subparallel to the original slope angle, with the possibility for a traffic layer at the top (Nichols, 1987; McLemore et al., 2005).

Recent concerns regarding rock pile stability have lead to the instigation of a multi-disciplinary research program to investigate the characteristics and behavior of the piles. Weathering of the mined rock containing varying amounts of pyrite could, over the long term, affect the rock pile's mechanical properties. The analysis of the structural (i.e. layered) characteristics of the rock pile material forms an important part of this program because of close connections that exist between the pile structure and geotechnical and chemical characteristics.

One traditional method for the characterization of rock pile properties includes drilling and core logging. These methods have the disadvantage of being expensive and they give only localized information. A variety of surface geophysical techniques have been proposed and used to characterize structural and geotechnical properties of slope material (Bogoslovsky et al., 1977; Bruno et al., 1998; Hack, 2000; Williams and Pratt, 1996) and reclaimed mining lands (Branson et al., 2000). Surface geophysical methods allow for non-intrusive characterization and imaging of the subsurface properties and can overcome some of the drawbacks of traditional methods for characterizing these materials. With the introduction of inexpensive computer power in the last two decades surveys have become cheaper and easier to perform, and interpretations are now more reliable and accurate (Hack, 2000).

Along transects in a grid on top of one of the rock piles in the Questa molybdenum mine two electromagnetic methods were used to characterize the properties and internal structure of the material. A frequency domain electromagnetic induction system was used to measure the spatial variability in electrical conductivity. The electrical conductivity is related to soil water content, water quality, texture, and mineralogy. A ground penetrating radar (GPR) system was also used to image the internal structures of the top 5 to 8 meters of the rock pile. In addition, 7 trenches were excavated for analysis of the stratigraphy along one of the geophysical transects .

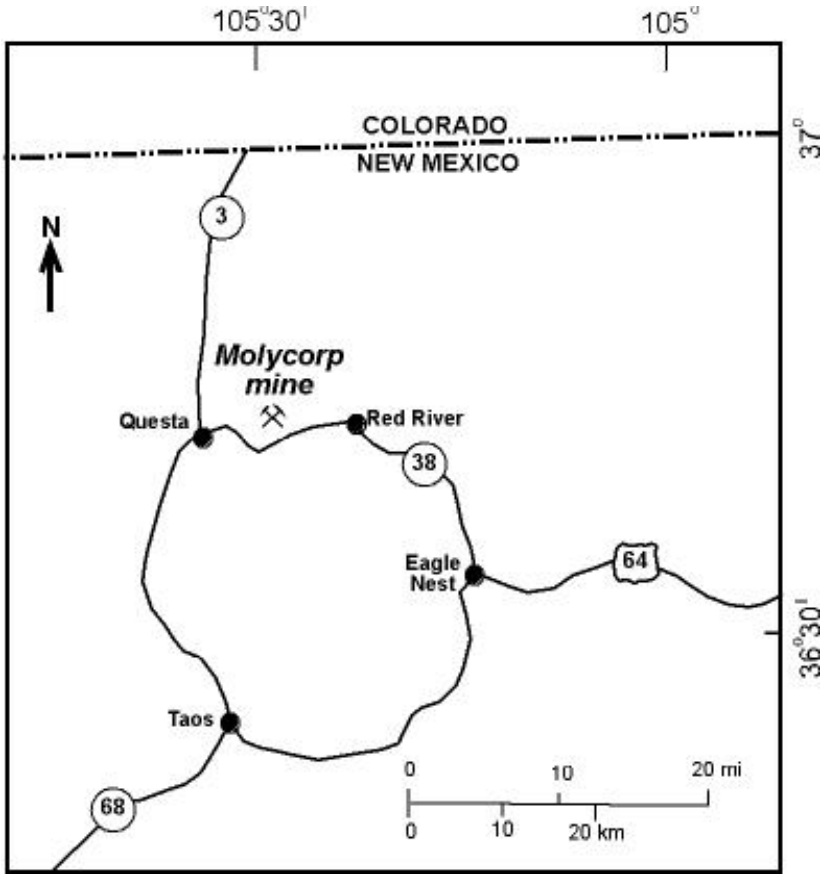


Figure 1. Location of Molycorp Questa mine, northern Taos County, New Mexico.

It is the purpose of this study (1) to demonstrate the applicability of near-surface geophysical methods for characterization of subsurface stratigraphy in general and (2) to improve the knowledge of the internal structure of the rock pile at Molycorp in particular. This manuscript describes the geophysical methods used, describes the survey layout used, and discusses the results of the research.

## Geophysical methods

Electromagnetic induction

Electromagnetic induction techniques measure the bulk electrical properties of the subsurface by generating electrical currents in the subsurface. In the transmitter coil an alternating electrical current generates a magnetic field. The magnetic field in turn generates a secondary electric field, the strength of which depends on the electrical conductivity of the subsurface. The primary factors affecting the electrical conductivity include clay content, clay type, water content, and solute content. A list of typical conductivity values for some common materials is given in Table 1. It must be noted that the material descriptions do not account for variations in clay content due to weathering, water saturation, or quantity of minerals in solution in water. These factors influence the conductivity values more than most of the material constituents.

In frequency domain EM induction techniques the distance between the coils and the frequency control the depth of investigation. This also allows for vertical profiling (depth sounding) and horizontal profiling. In vertical profiling, when the distance between the coils is

increased or the frequency is lowered then the received signal is more influenced by deeper buried materials (Borchers et al., 1997). In horizontal profiling, the coil distance is kept constant, and by taking readings at regular distances the lateral changes in (apparent) electrical conductivity can be measured. We used a Geonics EM31 frequency domain EM induction system, which operates at a frequency of 9.8 kHz, for lateral mapping of the conductivity variations. The EM31 is sensitive to conductivity variations up to a depth of approximately 6 meters.

Table 1. Characteristic values of physical properties of common earth materials (after Davis and Annan, 1989, and Van Overmeeren, 1991).

| Medium | Relative dielectric permitivitty ($\varepsilon_r$) | Propagation velocity (m/ns) | Attenuation (dB/m) | Electrical conductivity (mS/m) |
|---|---|---|---|---|
| Air | 1 | 0.3 | 0 | 0 |
| Dry sand | 4 | 0.15 | 0.01 | 0.1-10 |
| Water saturated sand | 25 | 0.06 | 0.03-0.3 | |
| Clays | 5-40 | 0.05-1.3 | 1-300 | 10-1000 |
| Fresh water | 80 | 0.034 | 0.1 | 0.1-30 |
| Saline water | 80 | 0.034 | 1000 | 4000 |

Ground penetrating radar (GPR)

GPR transmits short-pulse high-frequency electromagnetic waves into the subsurface that reflect off layers with contrasting properties. By recording arrival time and amplitude of reflected waves GPR allows for the rapid acquisition of high-resolution images of the sedimentary architecture in the shallow subsurface (Davis and Annan, 1989). The subsurface electromagnetic changes are typically caused by variations in water content that, in turn, are often the result of changes in textural properties related to layering (e.g., grain size distribution, porosity, packing, organic matter content). The amount of energy reflected by an anomaly or layer transition in the subsurface is proportional to the magnitude of the change in electromagnetic properties. By performing multiple measurements along a transect GPR generates a 2-dimensional cross section (Fig. 2).

The performance of GPR systems depends on the electromagnetic properties of the soil and the frequency used. Both the relative dielectric permittivity and the electrical conductivity have an important effect on the electromagnetic wave velocity and signal attenuation (Table 1). In material with a high electrical conductivity (e.g., significant amounts of clay and/or water) the signal attenuation is higher. The signal frequency has an effect on both penetration depth and resolution. Lower frequencies have the advantage of deeper penetration but with their larger wavelength they have a lower resolution (Table 2). In this study we used a commercially available pulseEKKO100 system from Sensors&Software, Canada, at two different antenna frequencies: 100MHz and 200MHz. The data were processed and imaged using standard software supplied by the manufacturer.

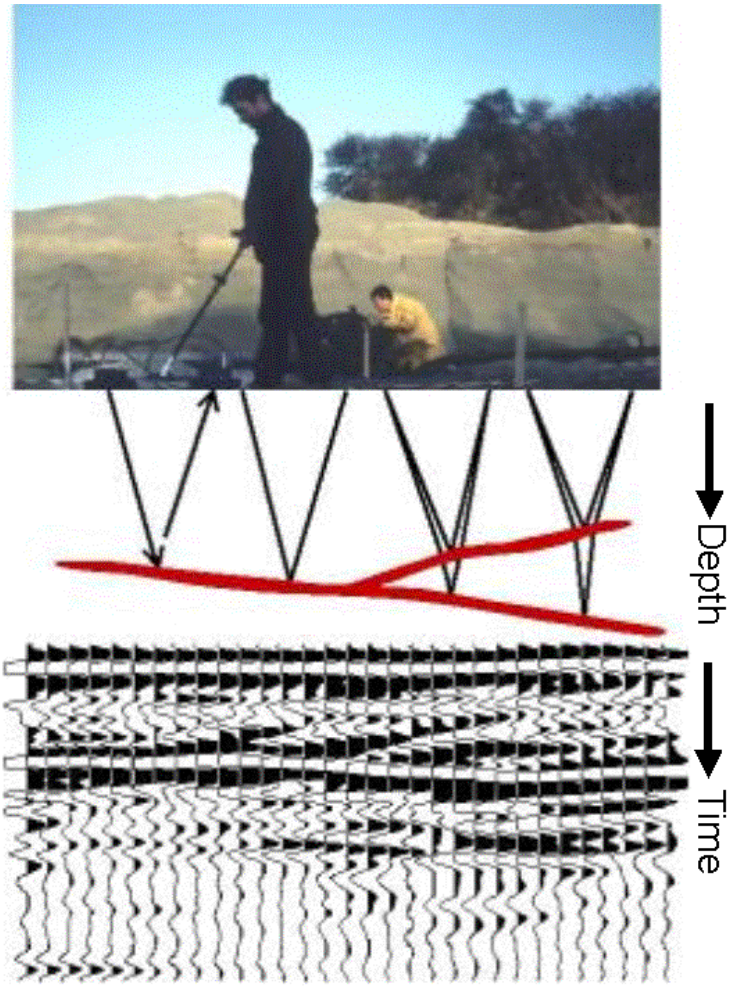


Figure 2. Operation principles of ground penetrating radar.

## Survey Layout

The survey layout on top of the Goathill North rock pile consists of 5 east-west transects perpendicular to the strike of the rock pile sediments and 1 north-south transect connecting these (Fig. 3). The 5 parallel transects start at the road, which borders the open pit, and end close to the crest of the rock pile where the (sub-)horizontal surface ends. The EM31 electromagnetic induction system was used to survey all 6 transects at a step size of 1m (Table 3). The GPR was used to survey all 5 east-west parallel transects at the lower frequency of 100 MHz. In addition, two east-west transects (Lines 4 and 5; see Fig. 3) were surveyed using higher frequency antennas of 200 MHz. Both frequencies were used to survey sections of the north-south transect (Line 6; Table 3). The GPR readings were collected at a station spacing of 0.1m.

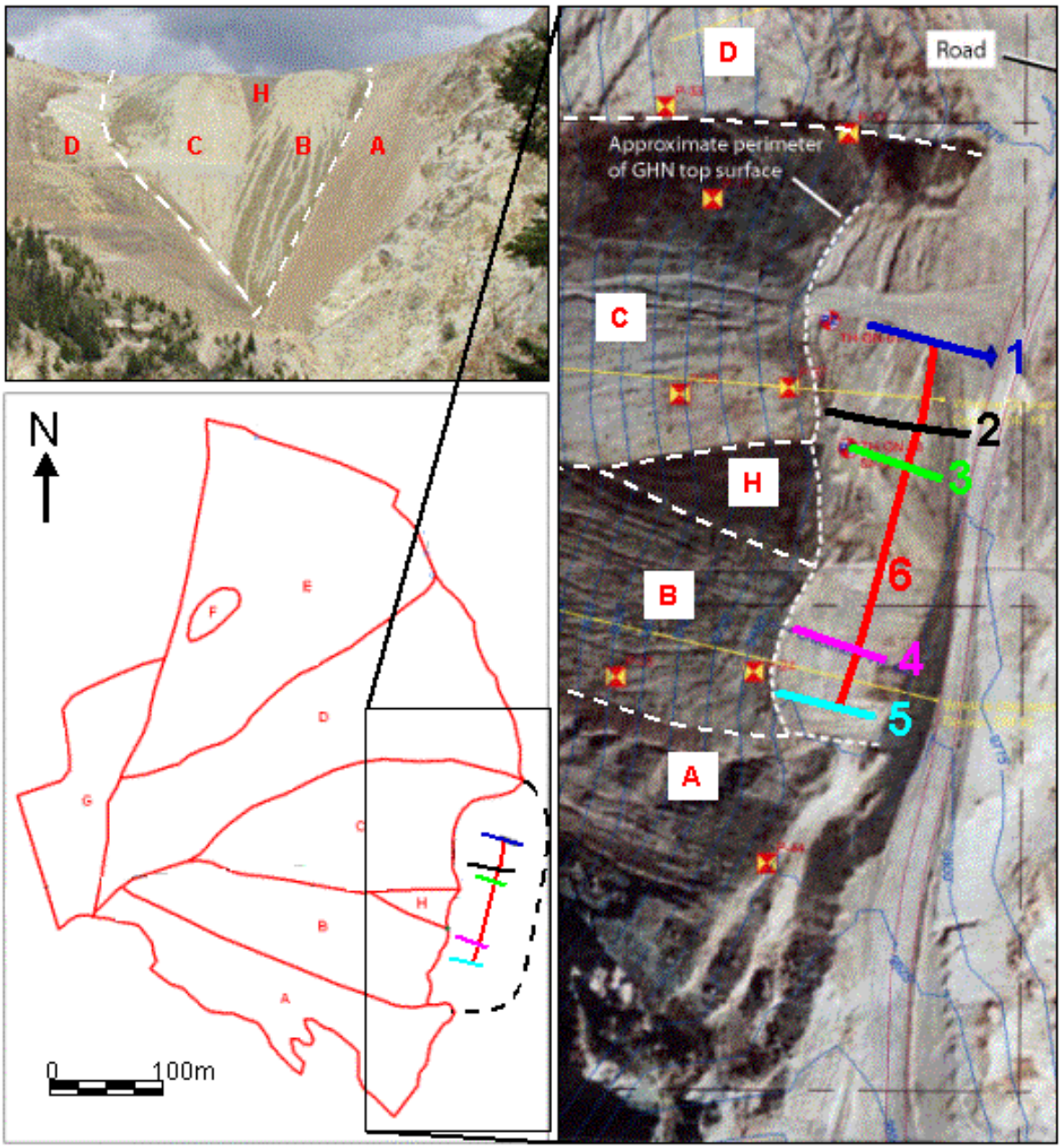


Figure 3. Setting of geophysical survey on the Goathill North (GHN) rock pile. Top left: picture of GHN rock pile, looking east. We studied the part of the rock pile between the dashed lines. The letters refer to distinct units on the geologic / structural map of GHN rock pile before regarding (lower left). A description of the units can be found in McLemore et al., 2005. The boxed area represents the aerial photograph (right), the Goathill North Drilling and Instrumentation Map (updated 10/06/03). The photograph shows the locations of geophysical survey lines (colored lines and numbers), relative to the different units of the rock pile (boxed letters). Data are based on GPS measurements on May 18 2004.

Table 2. Velocity (v) and wavelength (λ) of GPR waves in sand as a function of water saturation and commonly used GPR frequencies (after Van Dam and Schlager, 2000). Because the center frequency of GPR energy in geologic materials may be 20% lower than the in-air center frequency of a GPR antenna, the wavelength may be underestimated here (Lehmann and Green, 1999). The resolution can be approximated by a quarter of the wavelength (Van Dam et al., 2003).

| Frequency | Dry sand | | Moist sand | | Saturated sand | |
|---|---|---|---|---|---|---|
| (MHz) | v (m/ns) | λ (m) | v (m/ns) | λ (m) | v (m/ns) | λ (m) |
| 50 | 0.15 | 3 | ~0.1 | 2 | 0.06 | 1.2 |
| 100 | 0.15 | 1.5 | ~0.1 | 1 | 0.06 | 0.6 |
| 200 | 0.15 | 0.75 | ~0.1 | 0.5 | 0.06 | 0.3 |
| 450 | 0.15 | 0.33 | ~0.1 | 0.25 | 0.06 | 0.13 |

Table 3. Summary of geophysical measurements on GHN rock pile.

| Name | Length (m) | Intersection with Line 6 (in m) | Distance / position on Line 6 (in m) | Orientation | EM31 | GPR (100MHz) | GPR (200MHz) |
|---|---|---|---|---|---|---|---|
| Line 1 | 35 | 15 | 0 | E-W | × | × | – |
| Line 2 | 42 | 15 | 26 | E-W | × | × | – |
| Line 3 | 27 | 9 | 39 | E-W | × | × | – |
| Line 4 | 32 | 11 | 99 | E-W | × | × | × |
| Line 5 | 30 | 10 | 17 | E-W | × | × | × |
| Line 6 | 117 | – | – | N-S | × | × (0-39m) | × (99-117m) |

## Results

Electromagnetic induction

The electrical conductivity measurements range between 3 and 28 mS/m. There are significant variations in electrical conductivity between the northern and the southern parts of the Goathill North rock pile where the measurements were taken.

Fig. 4 shows the variation in electrical conductivity for the 3 survey lines on the northern part of the rock pile (see Fig. 3 for location). The electrical conductivity is fairly constant and fluctuates between 5 and 8 mS/m. However, Line 1 shows a steady decrease in conductivity followed by a sharp decrease in electrical conductivity between 30 and 35m. This pattern can be largely attributed to the local geomorphology of the pile. After approximately 10m from the start of the profile, the surface at Line 1 gradually inclines (this is due to bulldozer work), with a steepening slope towards the end. This higher topography leads to lower amounts of pore water, and consequently lower electrical conductivities.

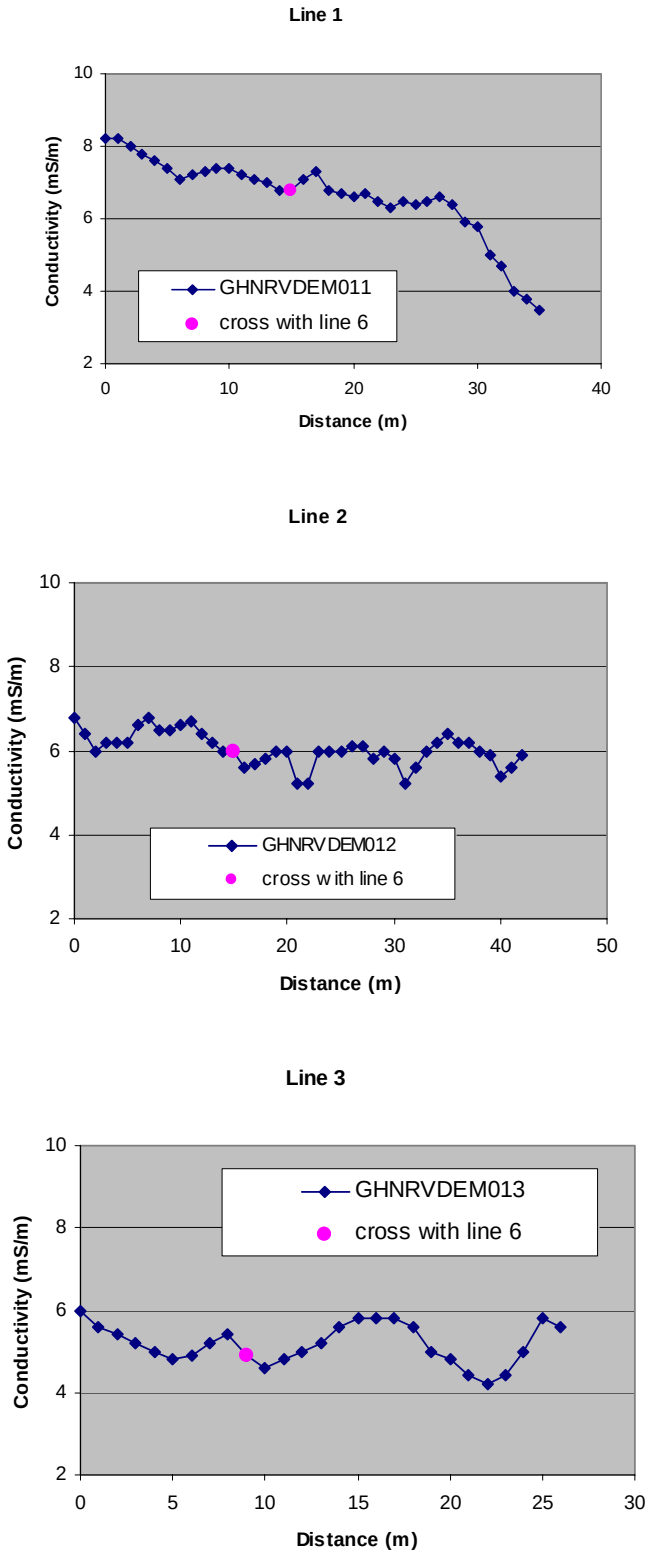


Figure 4. EM31 measurements for Lines 1-3 on the GHN rock pile. All profiles have been taken in an east (x=0m) to west direction.

The conductivity profiles for the southern part of the rock pile (Lines 4 and 5) show a different character than the northern part (Lines 1, 2, and 3). There appear to be significant differences between the road-side (east) and the crest-side (west) of the rock pile (Fig. 5) along Lines 4 and 5. The conductivity values for the road-side part of these transects (roughly between the start of the line and the intersection with Line 6; see Fig. 3) are on the same order as those in Lines 1-3. Westward of Line 6, the conductivity values show a steady increase towards 21 and 28 mS/m for Line 4 and Line 5, respectively. The slight decrease at the end of both lines is caused by metal poles and wires (located at the crest of the rock pile) that interfere with the magnetic field.

The increase in conductivity values between ~10m and the western end of Lines 4 and 5 cannot be explained by the local topography, because the surface slopes slightly off towards the east (i.e., the start of the lines), as well as to the north. For that reason it would be expected that this area is relatively dry and with lower conductivities. The unexpected high electrical conductivity values can be explained by:

i) A higher clay content. Clay has a larger water retention capacity than silts and sand. As a result, a higher clay content increases the gravimetric water content in the unsaturated zone. This can lead to higher values of electrical conductivity.

ii) A different mineralogy and pore water composition. The mineralogy can have an effect on the electrical conductivity, especially through its impact on the cation exchange capacity (CEC) and solute composition.

iii) A perched water table. An increase in water has a positive effect on the conductivity. A water table perched on an impervious layer can account for the observed effect.

Line 6 connects the 5 east-west trending profiles, and shows a trend of increasing values of electrical conductivity towards the south, with a peak around 90m (Fig. 6). Extrapolating the data in Lines 4, 5, and 6, we can identify an approximately 20x40m area in the southwestern part of the rock pile with anomalously high conductivity values.

Ground penetrating radar

Processing. The data were processed using a time-zero correction to line up the first arrivals. Also, a filter was applied for the removal of low frequency noise. Finally, by subtracting the average trace of the whole dataset from each individual trace the effect of the first arrivals (horizontal reflections in the top of the transects that result from energy traveling directly from the transmitting to receiving antenna) was reduced. A velocity of 0.1 m/ns was used to convert time into depth.

Display. In the display and interpretations of the survey lines color codes have been used to delineate reflection patterns and features.

Point reflectors either below (e.g., pipes, tunnels, or boulders) or above (e.g., metal objects) the ground surface cause hyperbolic reflections in the data. The apex of the hyperbolas is the point where the distance between the antennas and the point source was the shortest. The dip angles of the hyperbola asymptotes give an approximate estimate of the GPR wave velocity, which allows for distinguishing between below- (velocity < 0.15 m/ns) and above-ground

reflections (velocity in air = 0.3 m/ns). Hyperbolas and other artifacts have been highlighted in turquoise/blue.

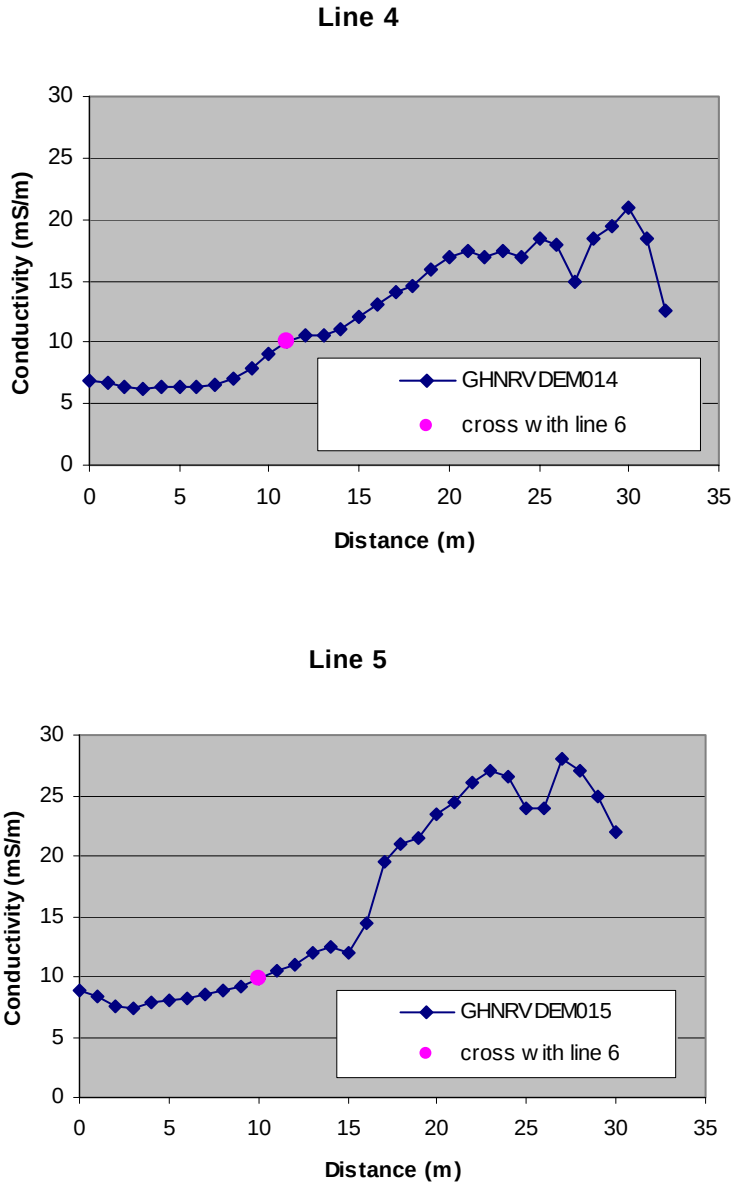


Figure 5. EM31 measurements for Lines 4 and 5 on the GHN rock pile. Both profiles have been taken in an east (x=0m) to west direction.

Sub-horizontal reflections and reflections dipping to the east occur in the road-side part of the east-west transects, and more in the 200 MHz than in the 100 MHz profiles. These reflections have been highlighted in yellow. Reflectors dipping towards the west have the same dip direction as the current slope of the rock pile. These dips reflect the depositional process (rock pile dumping) possibly in combination with secondary processes (e.g., weathering). These reflections have been highlighted in orange.

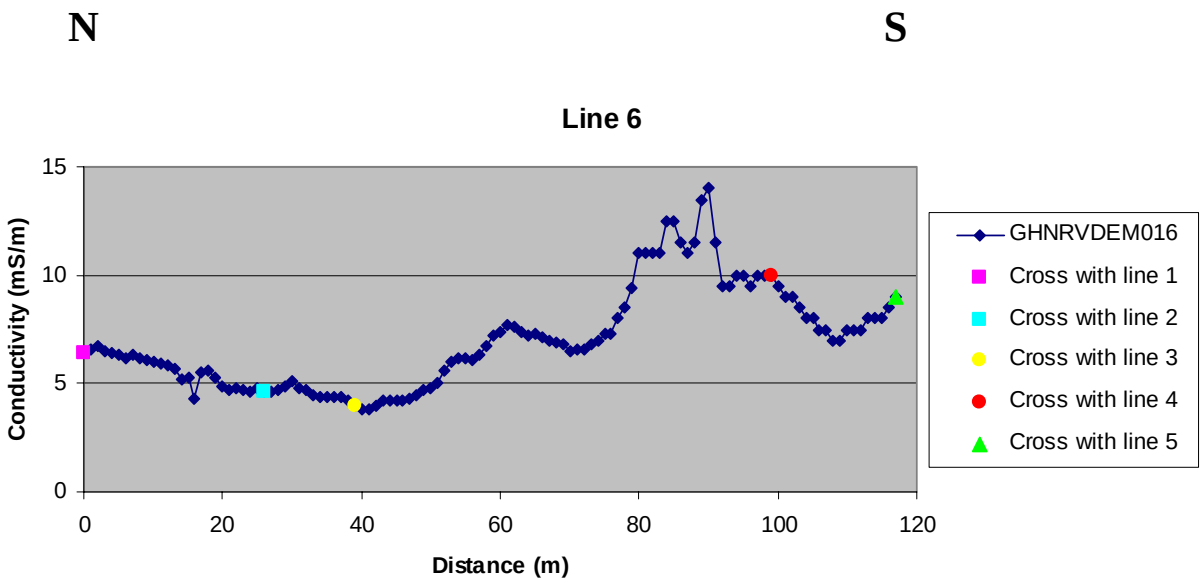


Figure 6. EM31 measurements for Line 6 on the GHN rock pile. The profiles runs from north (x=0m) to south

Faults or cracks are visible through the lateral discontinuity in GPR reflections. Locations of possible dislocation features have been highlighted using a green line. Sub-horizontal reflections and convex structures in the north-south trending profiles can be related to depositional lobes. These structures have been highlighted in pink.

Interpretation. The three GPR sections on the northern part of the Goathill North rock pile (Lines 1, 2, and 3) are dominated by reflections dipping to the west (Figs. 7 and 8). The reflections can be traced to a maximum depth of 4.5 to 5 meters. However, these depths can vary, as the velocity that was used for the time-to-depth conversion may not be perfect. Using the current depth scale the maximum angle for these reflectors is about 30º. However, the dip angles are not consistent, which indicates that not all material was deposited under similar conditions and not all was deposited at the angle of repose. The north-south trending transect (Line 6) that connects Lines 1, 2, and 3 shows no clear reflection pattern and reflections in this section can not be tied in with those in Fig. 7 and 8. Part of this can be due to the large step size (0.25m) as compared with the east-west transects (0.1m) and resulting aliasing problems.

The GPR sections for Line 4 and 5 were surveyed using both 100 MHz and 200 MHz antennae. These transects show a somewhat chaotic reflection pattern in the eastern part of the transects. This chaotic pattern (a mix of reflectors dipping to both left and right) is most prominent in Line 4 (Figs. 9 and 10). This irregular reflection pattern can be explained by i) an irregular subsurface stratigraphy, possibly due to ground work associated with construction of the road, which runs on an elevated berm here, or ii) interfering hyperbolas originating in the numerous surface and subsurface artifacts (see Fig. 11 for the metal poles and concrete blocks next to Lines 4 and 5). In Line 5 there are a couple of prominent westward dipping reflectors that can be tracked to a depth of approximately 6m in the 100 MHz survey (Fig. 12).

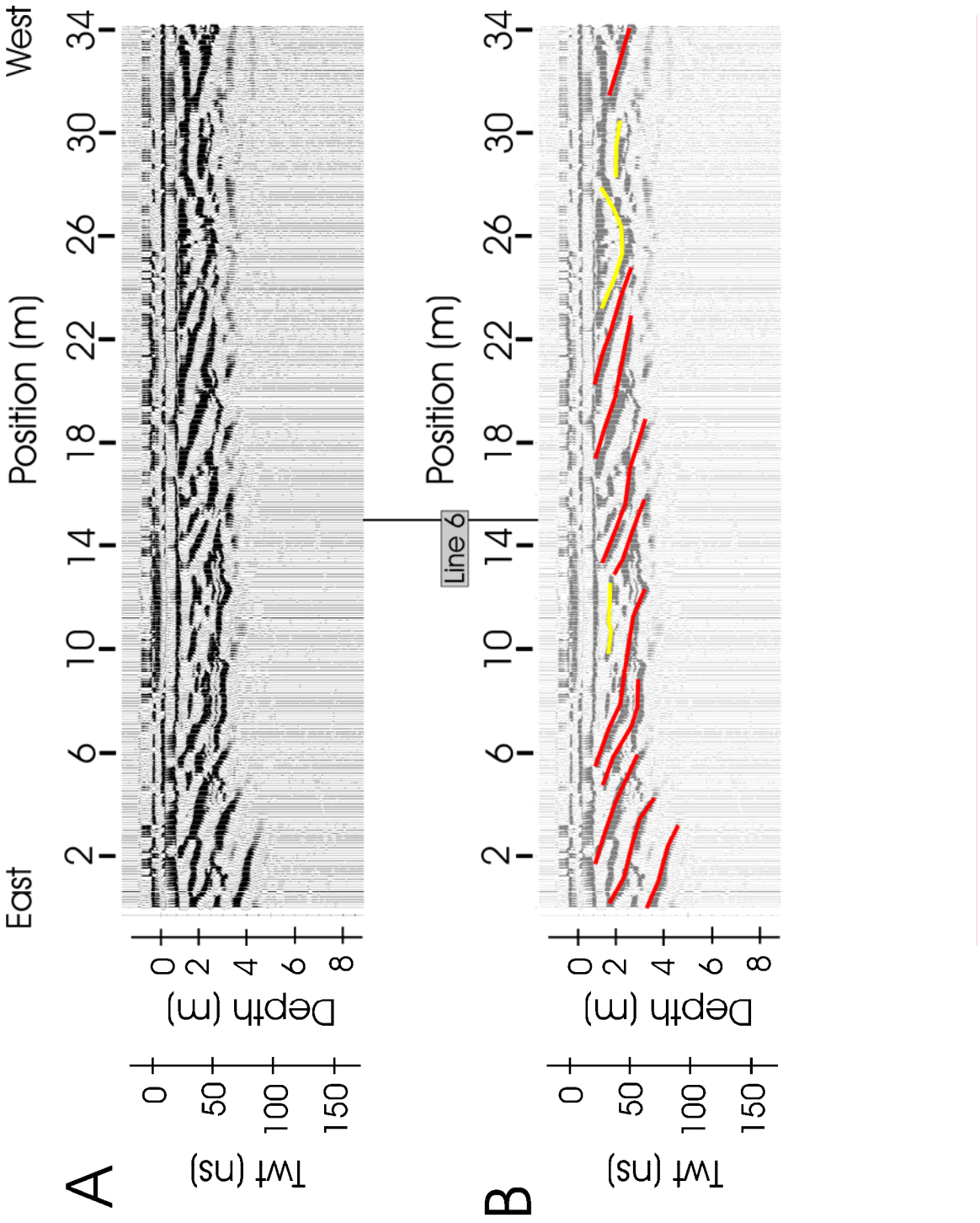


Figure 7. 100 MHz GPR Line 1 on the GHN rock pile. A) original transect after application of "dewow" filter, 1st pick, 1st shift, and removal of average trace. B) interpretation of original transect. Both transects use automatic gain control, magnitude 100, trace-to-trace average of 2, and time-to-depth conversion based on a velocity of 0.1 m/ns.

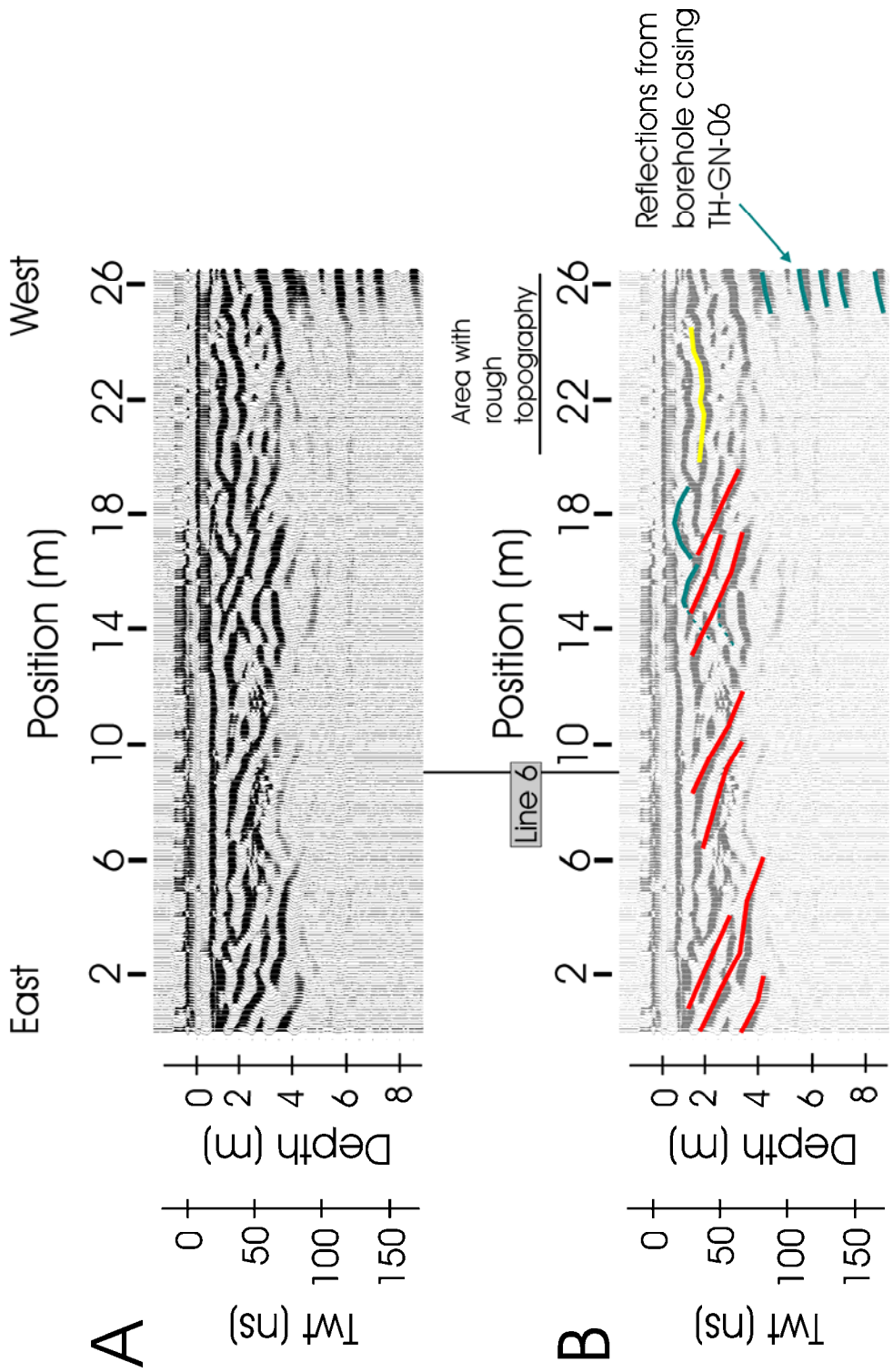


Figure 8. 100 MHz GPR Line 3 on the GHN rock pile. A) original transect after application of "dewow" filter, 1st pick, 1st shift, and removal of average trace. B) interpretation of original transect. Both transects use automatic gain control, magnitude 100, trace-to-trace average of 2, and time-to-depth conversion based on a velocity of 0.1 m/ns.

In the zone between approximately 15 and 30m in both Line 4 and Line 5 the reflection character is dominated by continuous sub-horizontal reflectors. The reflection at around 50 ns in the 100MHz survey of Line 4 (Fig. 9) suggests that there is a (perched) water table present between 2 and 3m depth in this area. In both 200 MHz surveys (Figs. 10 and 13) the penetration depth in the western part of the lines is significantly less that in the eastern (road-side) part of the lines. Because radar-wave attenuation is strongly dependent on the electrical conductivity function the lower radar-wave penetration ties in well with the high electrical conductivities that were found in this area (Fig. 5).

The north-south trending Line 6 (200 MHz; Fig. 14) shows clear sub-horizontal and convex reflections. At the intersection of Lines 5 and 6 the travel times of the reflections in both lines match very well. At the intersection of Lines 4 and 6 reflections of subsurface structures in Line 4 are obscured by multiple hyperbolic reflections and, consequently, the travel times of the reflections in both lines do not fit.

## Trench

Trench LFG003 has been excavated along part of Line 1 to analyze the subsurface stratigraphy and to compare the results with the GPR survey of the same transect (Fig. 7). To ensure that lateral variation in stratigraphy plays a minor role in the description of the trench walls and comparison with the GPR data, the trench has been excavated in four consecutive steps. After opening of the first bench, with a width of approximately 2 meters, the wall was described and samples were collected. Next, the first bench was widened and a second bench was excavated. This process was repeated until four benches, reaching a maximum depth of 4.6 meters, were excavated (Fig. 15). The described walls were always on the northern side of the trench and were never more than around 1 meter away from the centerline below Line 1.

Figure 16 presents the stratigraphic interpretation of the trench walls and the comparison with the GPR data. A total of 7 Units have been identified in the trench using visible structural features, color, and texture (Fig. 16B). For each layer several characteristics, such as the consistency, moisture content, cementation, and rock lithology were identified (McLemore et al., 2005). Also, samples were collected for analysis of grain-size distribution, moisture content, chemistry and mineralogy. The layer texture varies from fine-grained to coarse; Units N and M1 are open framework gravels (cobble layers). The layer boundaries were generally well defined, but in some cases, especially where layers were thin, boundaries could not be traced from bench to bench. In the eastern part of the trench the layers dip at an angle of approximately 30 degrees. In the central part of the trench the layers dip at moderate angles. There is an angular inconformity between the cobble layer in the second bench and Unit K below and to the east of it. In the western part of the trench, the layers seem to return to a steeper shape.

Figure 16C presents an overlay of the interpretations of the trench statigraphy and the GPR reflection stratigraphy. Both interpretations that have been derived and produced independently show a remarkable similarity. In the eastern part of the transect, the top and bottom boundary of Unit M, dipping at approximately 30 degrees, have been very well imaged using GPR. Also the thin Unit W that starts in bench 2 and extends down into bench 3 is well represented in the GPR data; the resolution of the GPR signal is too low to image the top and bottom boundaries of this layer. The area with the sub-horizontal Unit N in the second bench is fairly well represented in the GPR data. In this area, the GPR reflection stratigraphy shows several gently dipping

reflections. The reflection from the top of Unit N is very clear and represents the transition from the compacted material to Unit N. The reflections and the lower boundary of Unit N do not exactly overlap. The lateral offset between the GPR line and the trench wall can be a cause for this and other misfits.

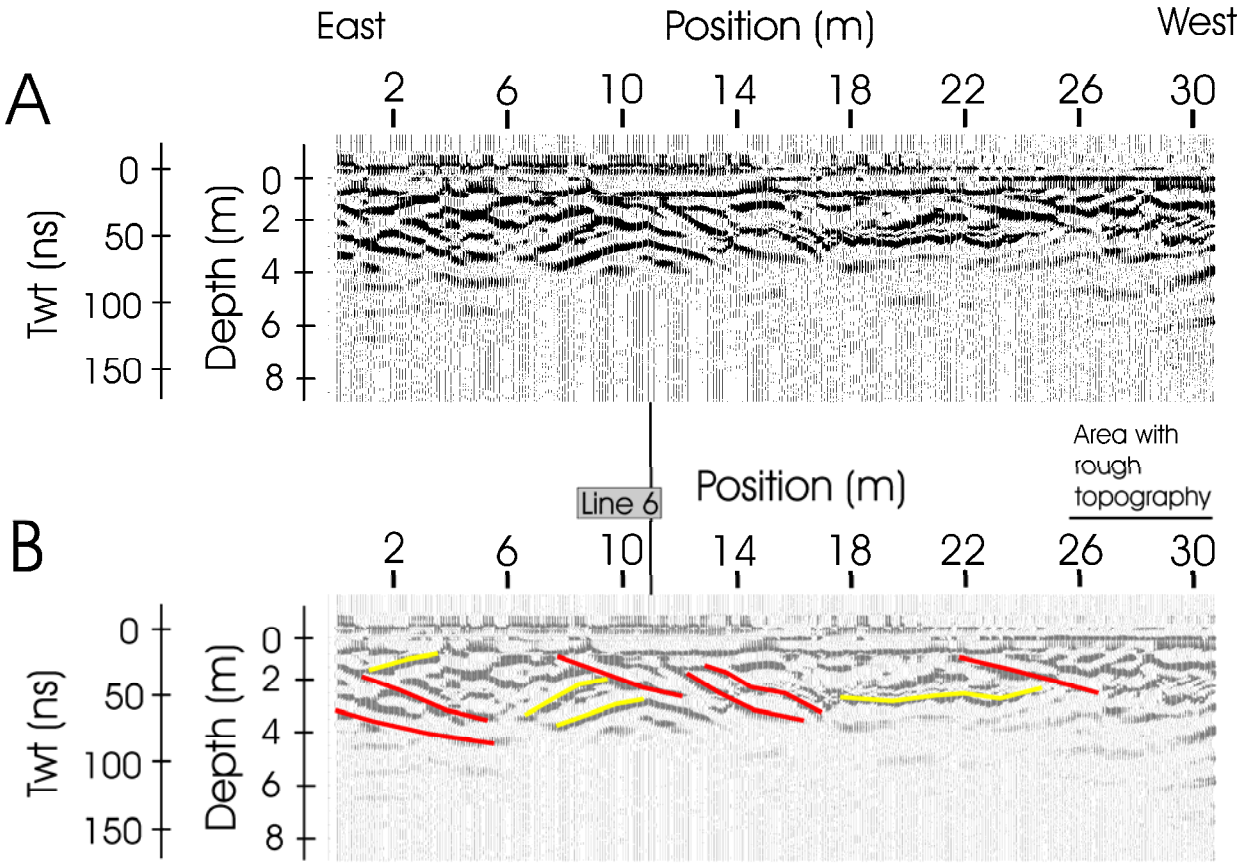


Figure 9. 100 MHz GPR Line 4 on the GHN rock pile. A) original transect after application of "dewow" filter, 1st pick, 1st shift, and removal of average trace. B) interpretation of original transect. Both transects use automatic gain control, magnitude 100, trace-to-trace average of 2, and time-to-depth conversion based on a velocity of 0.1 m/ns.

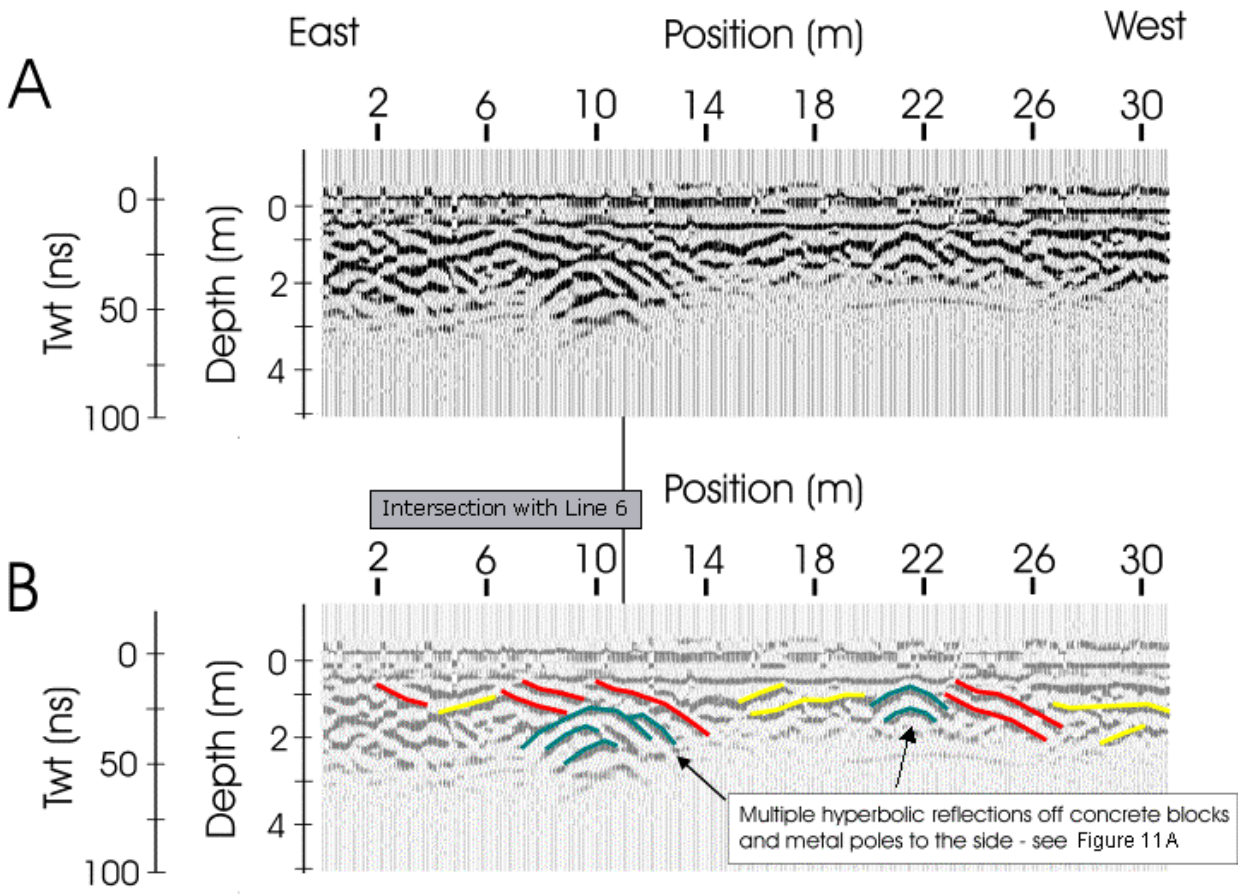


Figure 10. 200 MHz GPR Line 4 on the GHN rock pile. A) original transect after application of "dewow" filter, 1st pick, 1st shift, and removal of average trace. B) interpretation of original transect. Both transects use automatic gain control, magnitude 100, trace-to-trace average of 2, and time-to-depth conversion based on a velocity of 0.1 m/ns.

A

B

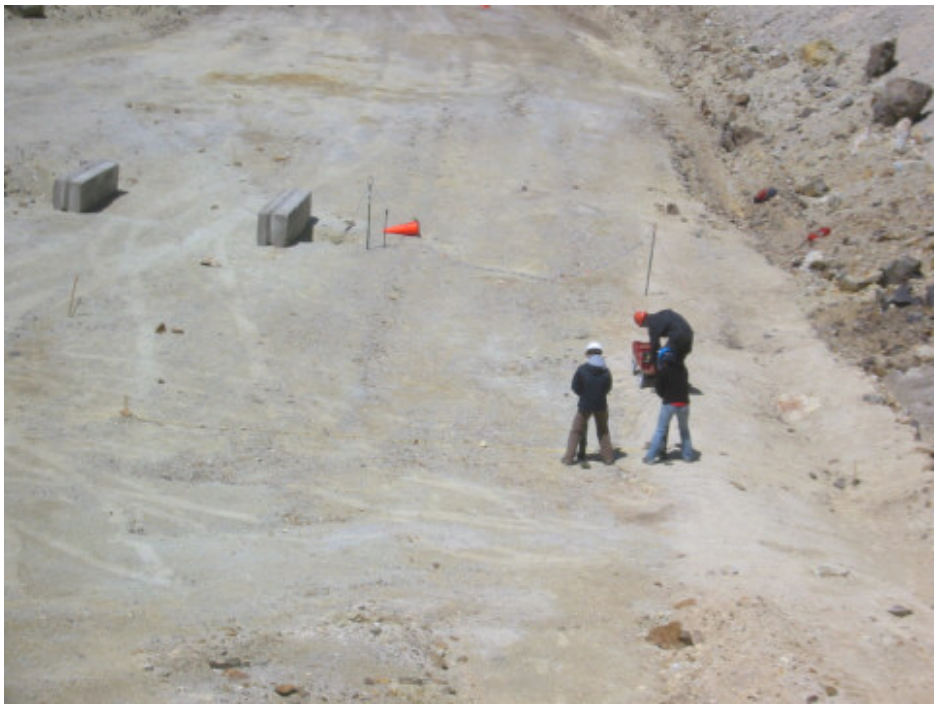

Figure 11. Pictures of Line 4, looking west (A), and Line 5, looking north (B).

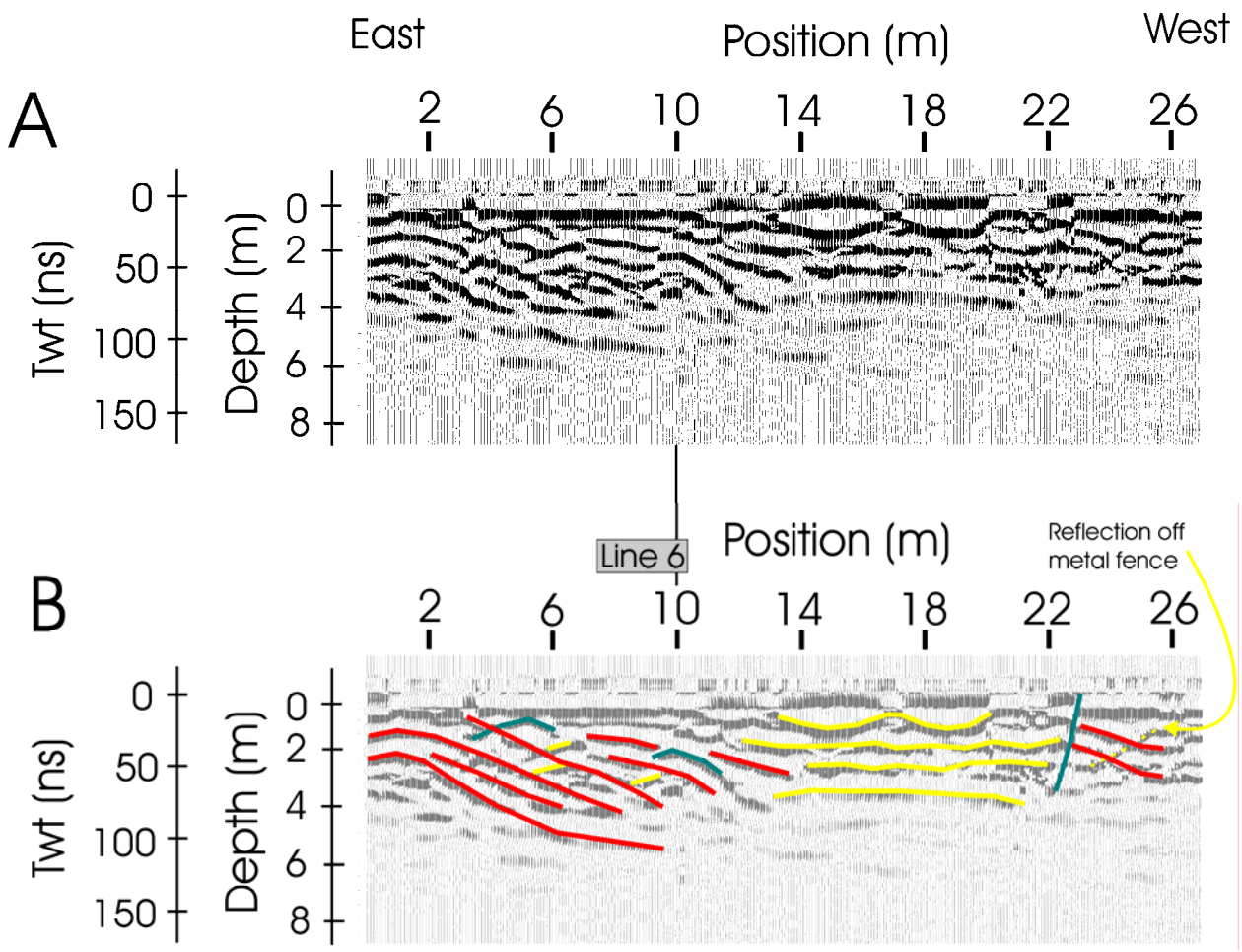


Figure 12. 100 MHz GPR Line 5 on the GHN rock pile. A) original transect after application of "dewow" filter, 1st pick, 1st shift, and removal of average trace. B) interpretation of original transect. Both transects use automatic gain control, magnitude 100, trace-to-trace average of 2, and time-to-depth conversion based on a velocity of 0.1 m/ns.

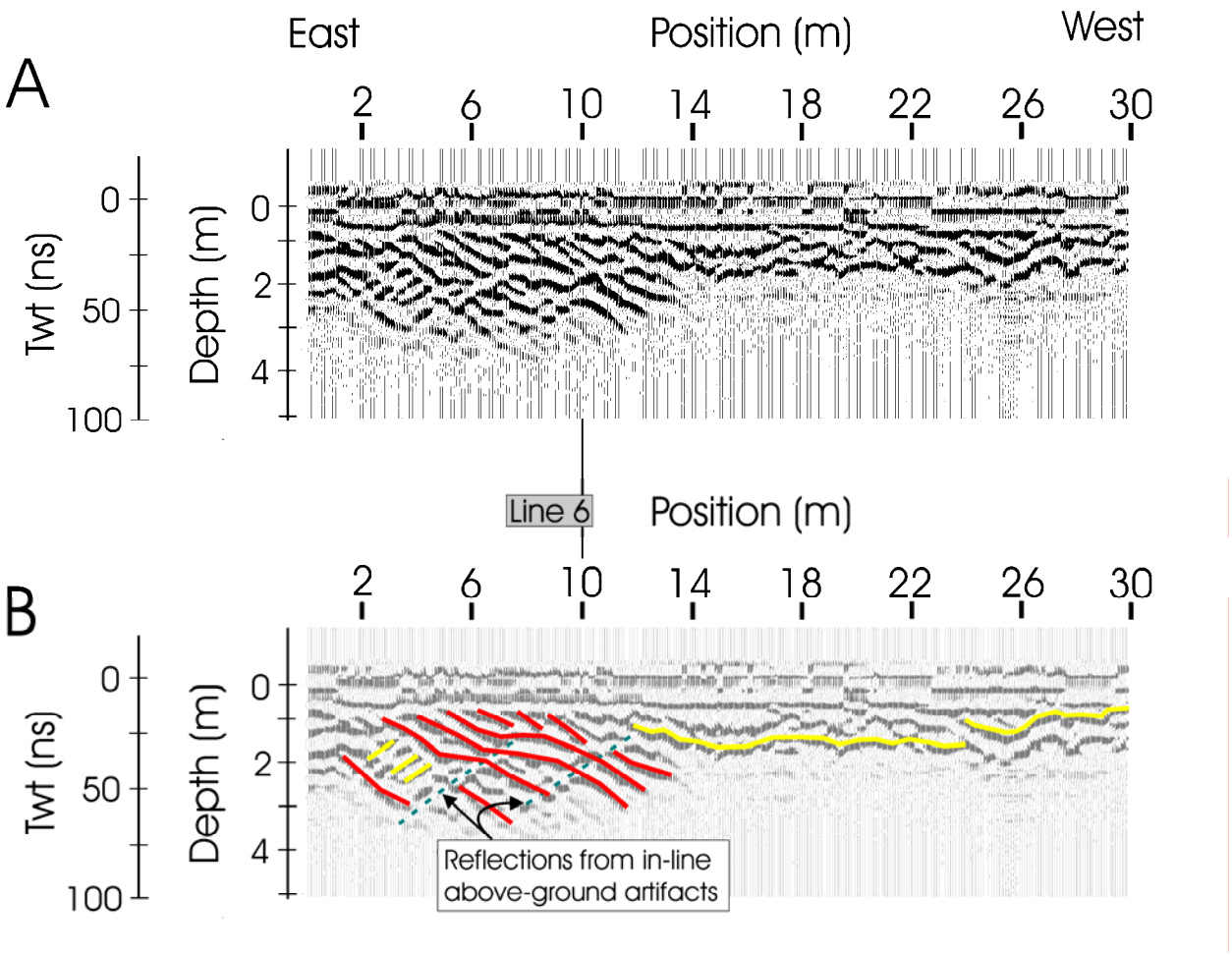


Figure 13. 200 MHz GPR Line 5 on the GHN rock pile. A) original transect after application of "dewow" filter, 1st pick, 1st shift, and removal of average trace. B) interpretation of original transect. Both transects use automatic gain control, magnitude 100, trace-to-trace average of 2, and time-to-depth conversion based on a velocity of 0.1 m/ns.

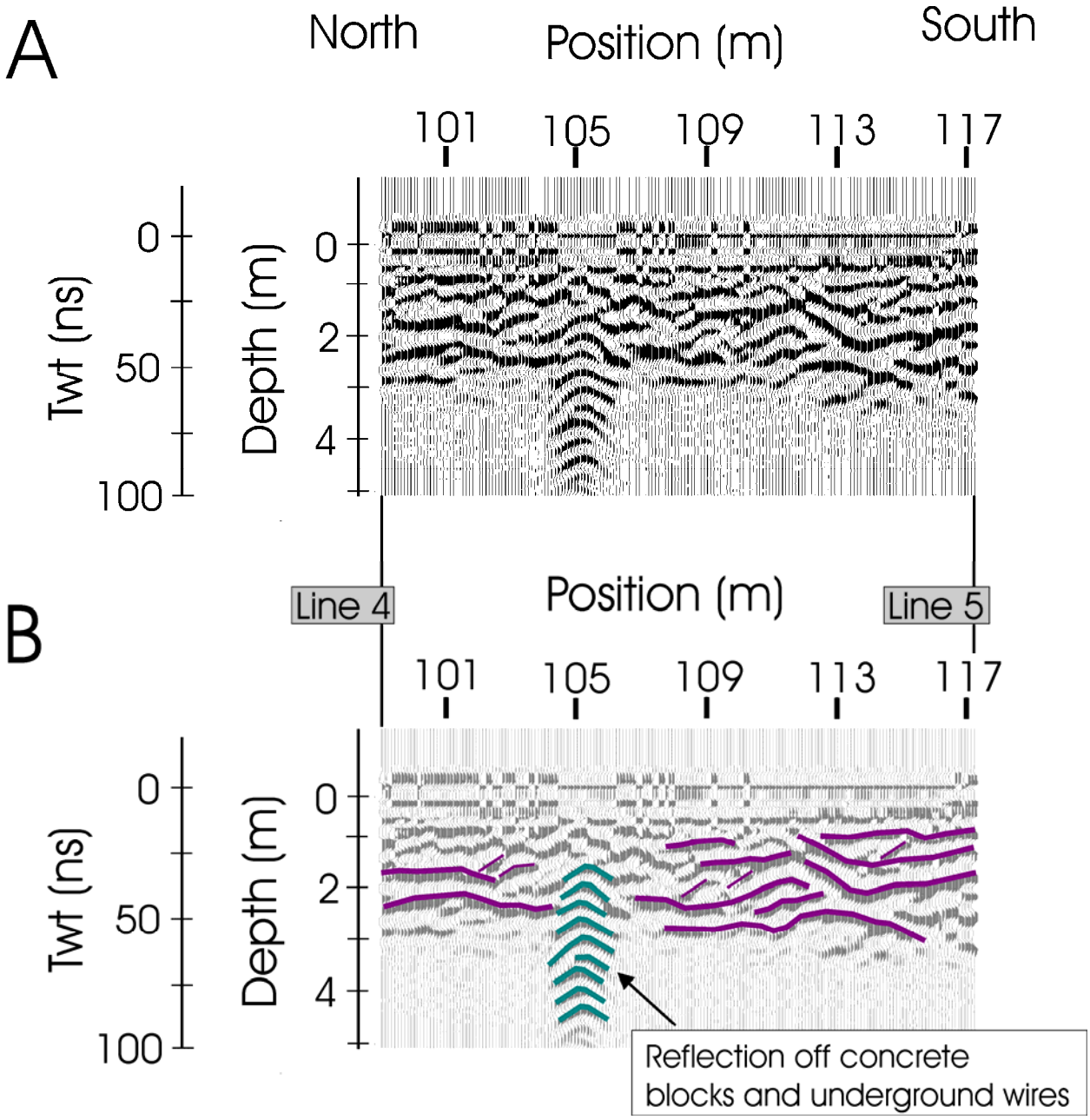


Figure 14. 200 MHz GPR Line 6 on the GHN rock pile. A) original transect after application of "dewow" filter, 1st pick, 1st shift, and removal of average trace. B) interpretation of original transect. Both transects use automatic gain control, magnitude 100, trace-to-trace average of 2, and time-to-depth conversion based on a velocity of 0.1 m/ns.

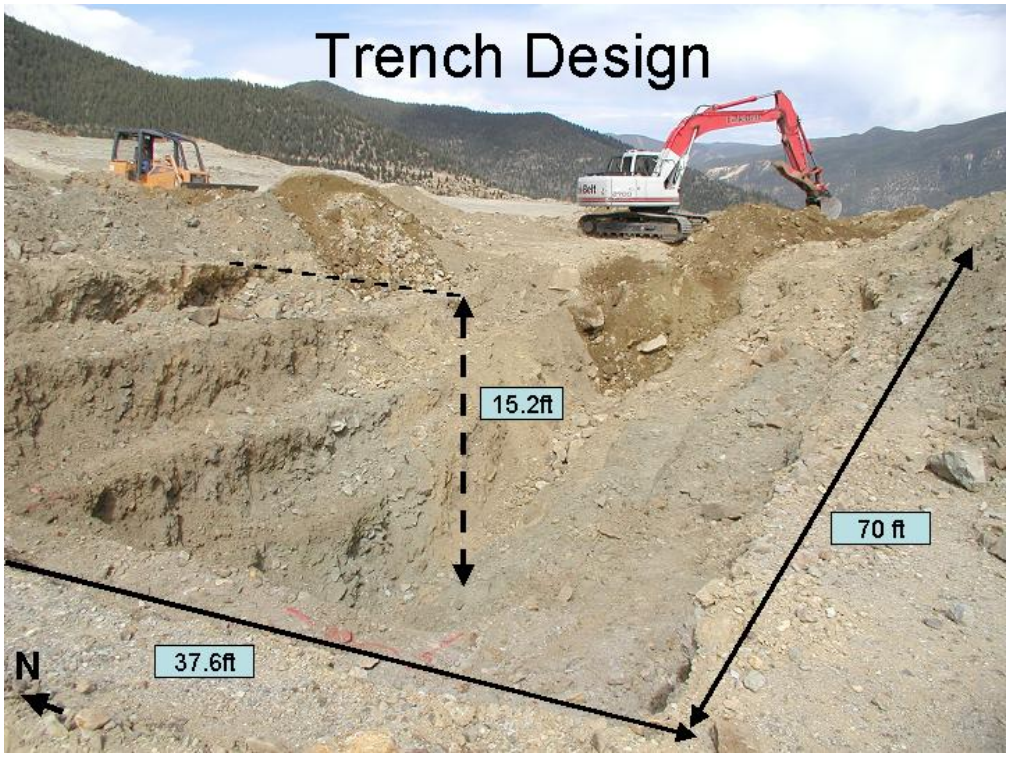


Figure 15. The design and dimensions of trench LFG003. The trench consists of a total of 4 benches up to a maximum depth of 4.6 meters.

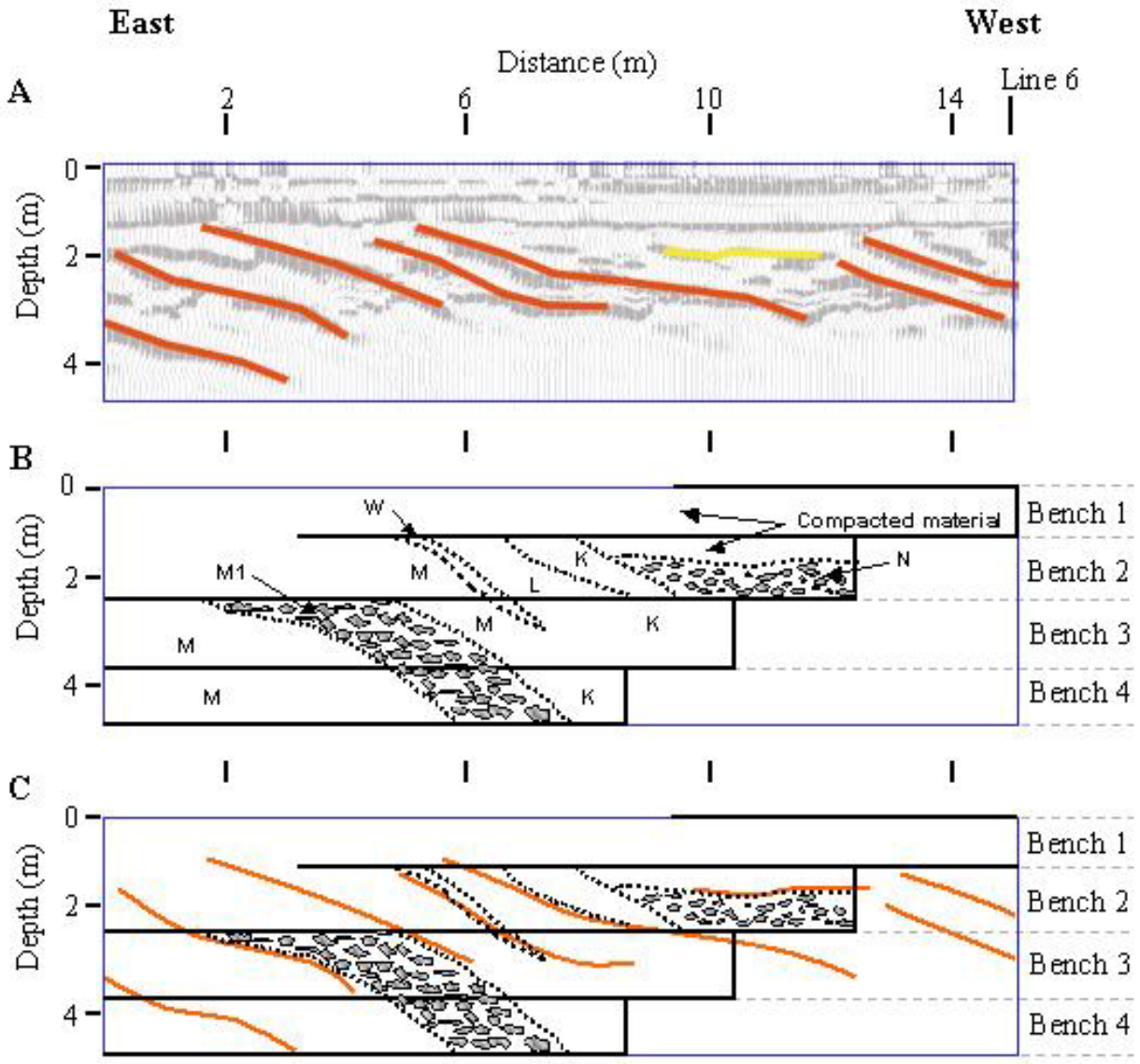


Figure 16. Comparison of the 100MHz GPR survey of Line 1 and the description of trench LFG003 that was excavated over part of Line 1. A) GPR data and interpretation of reflections. The blue box represents the approximate outline of the trench. B) Description of the layers identified in the trench; for a detailed description of the trench units see text and McLemore et al. (2005). C) Overlay of the GPR interpretation (in red) and the layers identified in the trench.

## Discussion and conclusions

This study demonstrates the application of near-surface geophysical techniques for the characterization of rock pile stratigraphy in general. These methods provide insight into the internal structure of a portion of the Goathill North rock pile at Molycorp's Questa mine. Along

a grid on top of Goathill North rock pile, electromagnetic induction and ground penetrating radar data were collected. Several conclusions can be drawn from the fieldwork.

The fieldwork showed that electrical conductivities vary between 4 and 30 mS/m. Using soil moisture and textural information from the trenches it can be possible to extrapolate these numbers to through the entire stable rock pile. For the largest part of the survey, the electrical conductivities are fairly constant around a value of 6 mS/m. However, one area (roughly 20 x 40m) in the southwestern part of the rock pile is characterized by significantly higher conductivities. Neither the topography nor other surface features suggest anything unusual. The GPR confirms the EM31 observations of this area with high conductivities. Firstly, the high electrical conductivities lead to a larger signal attenuation and cause a significant reduction in the penetration depth of the radar waves. Secondly, the GPR data are dominated by sub-horizontal reflections here, which suggest that this area has a different subsurface architecture than the rest of the rock pile. The anomalous electrical conductivity values and different GPR signature are most likely explained by the presence of a hard-pan or traffic layer due to bulldozer work or other re-grading work.

The GPR survey imaged the rock pile stratigraphy up to a depth of around 5 meters. Although this is significantly less than what can be achieved under ideal conditions (the maximum depth of penetration of GPR signals is limited by water and especially clay), the data show that GPR is an excellent means for characterizing the shallow subsurface stratigraphy. The excellent agreement between the stratigraphy observed in the trench and the GPR data further shows the applicability of GPR for imaging the rock pile stratigraphy.

The GPR reflection stratigraphy shows a general character of reflectors dipping to the west. These dips reflect the depositional process (rock pile dumping). Also secondary processes such as weathering can account for some of the reflections. GPR data can be more easily obtained than information from trenches, the data collection is cheaper, and using a densely spaced grid it is possible to obtain a semi-3D characterization of the variability. Last but not least, the information from GPR surveys can be used for input into geotechnical and hydrological models to improve understanding of the rock pile stability and behavior.

## Acknowledgements

This project was funded by Molycorp, Inc. and the New Mexico Bureau of Geology and Mineral Resources (NMBGMR), a division of New Mexico Institute of Mining and Technology (New Mexico Tech). We would like to thank Heather Shannon, Nathan Wenner, Samuel Tachie-Menson, John Sigda, and other professional staff and students of the large multi-disciplinary field team for their assistance in the fieldwork. We also would like to thank Jim Vaughn, and Mike Ness of Molycorp, Inc. for their training and assistance in this study. This paper is part of an on-going study of the environmental effects of the mineral resources of New Mexico at NMBGMR, Peter Scholle, Director and State Geologist. This manuscript was reviewed by one anonymous reviewer, whose comments were very helpful to improve the paper.

## References


Bogoslovsky, V.A. and Ogilvy, A.A. 1977. Application of geophysical methods for the investigation of landslides. Geophysics 42, 562–571.

Borchers, B., Uram, T., and Hendrickx, J.M.H. 1997. Tikhonov regularization for determination of depth profiles of electrical conductivity using non-invasive electromagnetic induction measurements. Soil Science Society of America Journal 61, 1004-1009.

Branson, J.L., Ammons, J.T., Freeland, R.S., Leonard, L.L., Stevens, V.C., Walker, D.S., and Yoder, R.E. 2000. Application of non-intrusive imaging in mapping perched water on reclaimed lands. Tennessee ASAE State Section Meeting, Martin, Tennessee, May 23, 2000.

Bruno, F., Levato, L. and Marillier, F. 1998. High-resolution seismic reflection, EM and electrokinetic SP applied to landslide studies: "Le Boup" landslide (western Swiss Alps)', Proceedings of the IV Meeting of the Environmental and Engineering Geophysical Society (European Section), Barcelona, pp. 571–574.

Davis, J.L. and Annan, A.P. 1989. Ground-penetrating radar for high resolution mapping of soil and rock stratigraphy. Geophysical Prospecting, 37, 531-551.

Hack, R. 2000. Geophysics for slope stability. Surveys in Geophysics 21, 423–448.

Lehmann, F. and Green A.G. 1999. Semiautomated georadar data acquisition in three dimensions. Geophysics. 64, 719-731.

McLemore, V.T.. Walsh, P., Donahue, K., Gutierrez, L.A., Tachie-Menson, S., Shannon, H.R., and Wilson, G.W. 2005. Preliminary status report on Molycorp Goathill North trenches, Questa, New Mexico. 2005 National Meeting of the American Society of Mining and Reclamation, Breckenridge, Colorado, June, this CD-ROM.

Nichols, R.S. 1987. Rock segregation in waste dumps. In: Proceedings of the International Symposium on Flow-Through Rock Drains, Cranbrook, British Columbia, September 8-11, 1986.

URS Corporation, 2000, Interim mine rock pile erosion and stability evaluations, Questa Mine, unpublished report to Molycorp, Inc., 6800044388.00, December 1, at www.molycorp.com.

Van Dam, R.L. and Schlager, W. 2000. Identifying causes of ground-penetrating radar reflections using time-domain reflectometry and sedimentological analyses. Sedimentology. 47, 435-450.

Van Dam, R.L., Van Den Berg, E.H., Schaap, M.G., Broekema, L.H. and Schlager, W. 2003. Radar reflections from sedimentary structures in the vadose zone. Geological Society of London, Special Publications 211, 257-273.

Van Overmeeren, R.A. 1994. Georadar for hydrogeology. First Break 12, 401-408.

Williams, R.A. and Pratt, T.L. 1996. Detection of the base of Slumgullion landslide, Colorado, by seismic reflection and refraction methods, in D.J. Varnes and W.Z. Savage (eds), The Slumgullion Earth Flow: A Large-Scale Natural Laboratory, U.S. Geological Survey Bulletin 2130, United States Government Printing Office, Washington.